LA-UR-14-20342
Approved for public release; distribution is unlimited.

Title: Characterization of the NPOD3 Detectors in MCNP5 and MCNP6

Author(s): Clark, Kimberly L.
Hutchinson, Jesson D.
Sood, Avneet

Intended for: Report

Issued: 2014-01-21

Characterization of the NPOD3 Detectors in MCNP5 and MCNP6

Kimberly Clark, Jesson Hutchinson, Avneet Sood

This work was supported by the DOE Nuclear Criticality Safety Program, funded and managed by the National Nuclear Security Administration for the Department of Energy.

Introduction

Researchers performed a series of measurements in May 2012 to characterize the NPOD3 detector systems. The detectors were placed in varying states of disassembly to determine the effect of individual components on detection efficiency. A 4.5 kg α-phase Pu sphere known as the Los Alamos BeRP Ball was used as the SNM source in both a bare configuration and reflected by varying thicknesses of polyethylene. A set of simulations matching the experimental setups were run and the data were compared to the measured data.

Description of Measurements

The BeRP ball was placed on an aluminum stand located on a steel cart. One NPOD3 detector sat at each end of the cart with the front face located 50 inches from the center of the BeRP ball as shown in Figure 1. One SNAP detector was positioned on an adjacent cart at 90 degrees from the NPOD detector plane. The distance between the center of the BeRP ball and the center of the He-3 tube in the SNAP was 100 inches.

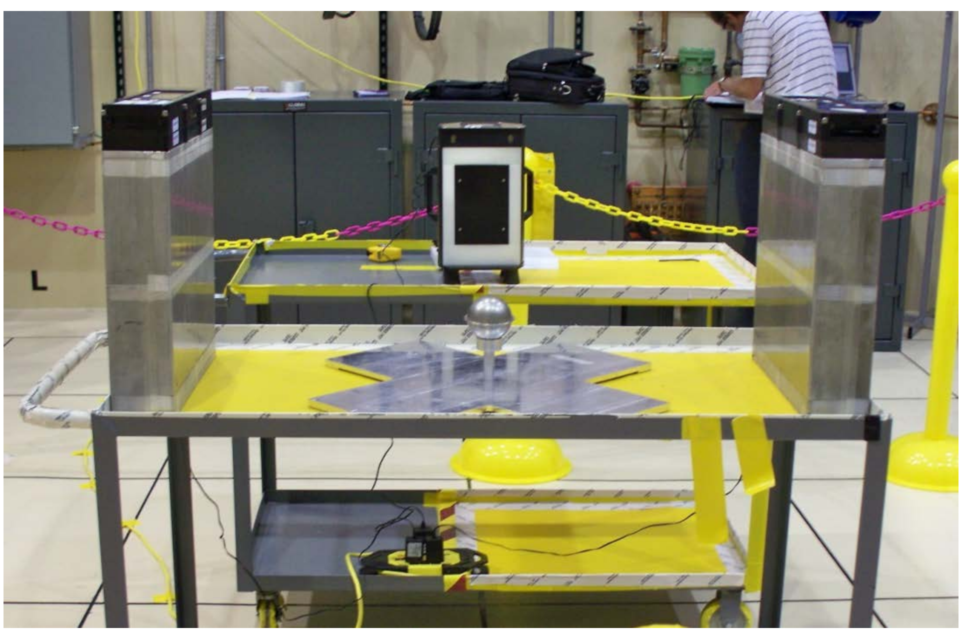

Figure 1: Default configuration: two NPOD3 detectors (left and right) and one SNAP detector (center, back) are used to measure the BeRP ball (center, front).

The configuration in Figure 1 was chosen as the default configuration. The subsequent configurations involved one NPOD in various stages of deconstruction and the SNAP with or without a front polyethylene shield (see Figs. 2 and 3).

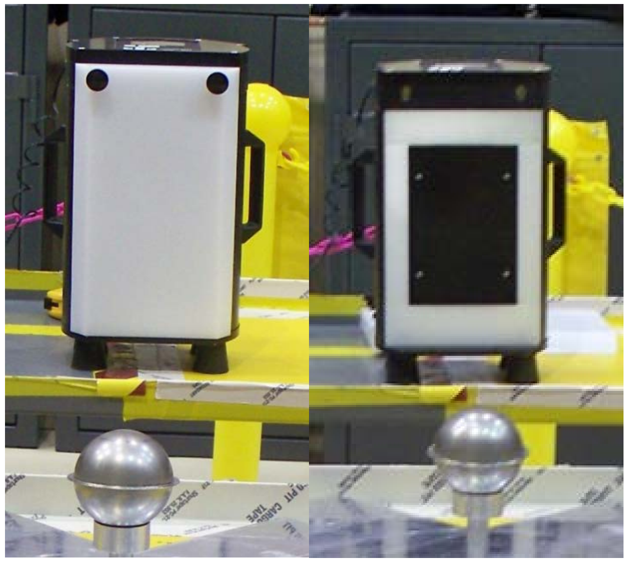

Figure 2: SNAP detector with polyethylene shield (left) and without.

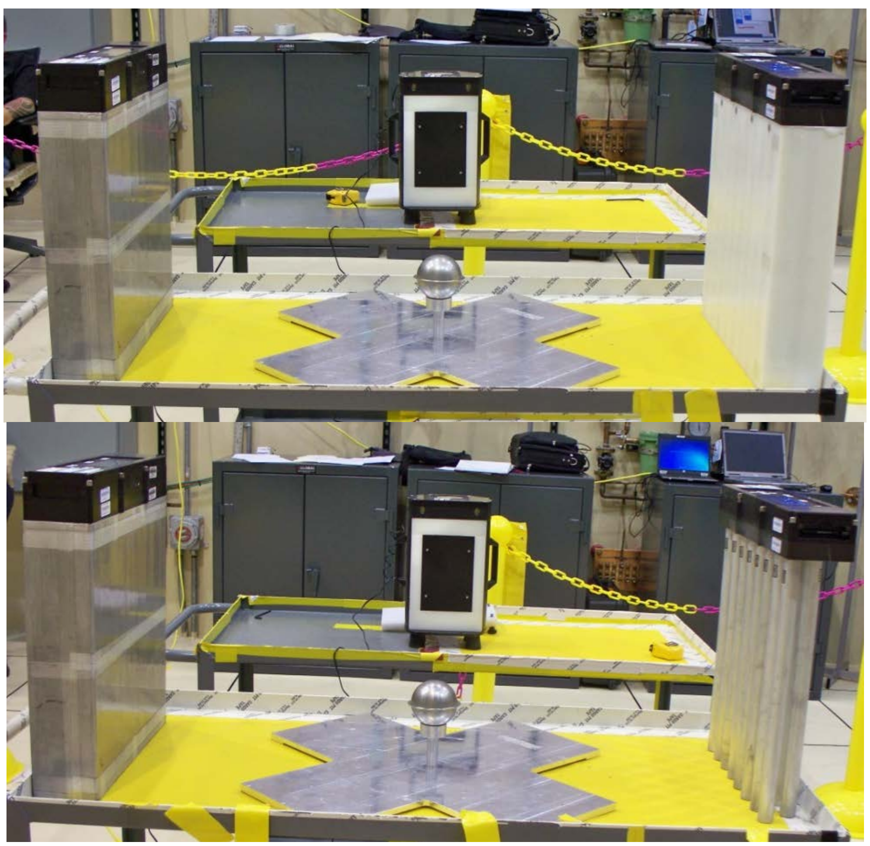

Figure 3: NPOD configurations - The NPOD on the left remained intact while the cadmium shield (top) and then the polyethylene moderator (bottom) were removed.

Table 1 lists the various NPOD3 configurations for the set of measurements (NPOD #1 is the NPOD3 on the left in Figure 1; NPOD #2 is on the right).

Table 1: List of detector configurations for the 2012 measurements.

Configuration	NPOD #1	NPOD #2	SNAP
1a	default	default	no poly
1b	default	default	poly
2a	blue cover	blue cover	no poly
2b	blue cover	blue cover	poly
3a	default	no cadmium	no poly
3b	default	no cadmium	poly
4a	default	no cadmium or poly	no poly
4b	default	no cadmium or poly	poly
5a	default	removed	no poly
5b	default	removed	poly
6	default	removed	removed
7a	default	removed	no poly, in line with NPOD
7b	default	removed	poly, in line with NPOD
8	default, 90 degrees	removed	removed
9a	default, 90 degrees	default, 90 degrees	no poly
9b	default, 90 degrees	default, 90 degrees	poly

The NPODs recorded list-mode data (time and location of detection events) and the SNAP measured a gross neutron count. The effective neutron source strength can be estimated from the SNAP counts.

The multiplication of the system is inferred using one of two formalisms of the Feynman variance method. The method is based on the fact that a random source, such as an (α,n) source, will have a Poisson distribution, while a correlated neutron source (a multiplying material) will have a distribution that deviates from a pure Poisson. The magnitude of this deviation provides insight into the multiplication of the material under analysis. Once the total multiplication of the system is obtained, the prompt multiplication factor can be inferred from Eq. 1:

$$k_p = 1 - \frac{1}{M_t} \qquad \text{Eq. 1}$$

Calculations

For each simulation, the same basic source and detector geometry models were used. The fission spectrum of the BeRP Ball source was defined using SOURCES4C, which accounted for the decay of radioisotopes [1]. Only the measurement times, source definitions and other data parameters particular to each code differed between the inputs.

The continuous-energy Monte Carlo codes MCNP5 with the LANL list-mode patch and the production code MCNP6.1, coupled with the ENDF/B VII.0 data libraries, were used to obtain simulated list-mode data to compare to the data from the measurements [2-4]. Unlike MCNP5 with the list-mode patch, MCNP6.1 does not have a straightforward way to provide list-mode data in the form desirable for multiplicity analysis with the in-house post-processing scripts. However, it can be extracted from a PTRAC (particle track) output file containing neutron capture information using a simple script. The resulting data are analyzed using the Hansen-Dowdy formalism of the Feynman variance method to obtain the total and leakage multiplication values and infer the effective multiplication factor of the system. Table 2 lists the parameters used in the calculation of the multiplication values for the bare system (the time of measurement was varied as necessary for the different measurements, but all other parameters remained constant for the bare system).

Table 2: List of parameters used in the calculation of the mutiplication values.

Param #	Description of Parameter	value
1	detector dead time (microsec)	2.5
2	time of measurement (seconds)	156
3	time bin width of detector (microsec)	256
4	neutron leakage from outermost surface (n/s)	1037264
5	id starter	Pu-240
6	0th order Divens (source) ~ Pu-240	1.769
7	id chain	Pu-239
8	1st order Divens (multiplier) ~ Pu-239	2.354
9	wt% of source ~ Pu-240	0.05954
10	#n/g-s emitted by SNM (Pu-240)	1020
11	neutron lifetime (seconds)	3.90E-05
12	non-correlated neutron source strength (n/s)	436.33
13	correlated neutron source strength (n/s)	282890
14	neutron leakage from SNM (n/s)	1037264

For the first set of calculations, which are described in this report, configurations 1, 3 and 4 (see Table 1) were modeled with the bare BeRP ball to verify that the detector models were accurately defined and to observe the differences in the results between the two codes. A previous comparison was done that showed good agreement between MCNP5 with the list-mode patch and MCNPX, which provides the same neutron capture tally PTRAC output option as MCNP6 [5].

Results

The total and leakage multiplication and the inferred k values were determined for both the simulations and the measurements. Table 3 shows a comparison of the results from MCNP6 and MCNP5 with the list-mode patch to the measured results. The count rates for the calculated results were obtained by dividing the total line count in the list-mode file (equivalent to the total number of absorptions in the NPOD detectors) by the total run time. The count rates are identical for both codes, and they both produce the same multiplicity and inferred k values regardless of measurement time as expected.

Table 3: Total and leakage multiplications and inferred k values for the simulated and measured data.

		MCNP6			MCNP5 w/patch			measured	
TIME (s)	CONFIGURATION (bare BeRP ball)	Ml	Mt	keff (inferred)	Ml	Mt	keff (inferred)	Mt	keff (inferred)
194	DEFAULT - Poly on SNAP	2.653	3.666	0.727	3.042	4.293	0.767	4.276	0.766
196	DEFAULT - Poly on SNAP	2.650	3.661	0.727	3.042	4.293	0.767	4.258	0.765
156	DEFAULT - NO Poly on SNAP	2.635	3.638	0.725	3.035	4.283	0.767	4.234	0.764
162	DEFAULT - NO Poly on SNAP	2.646	3.655	0.726	3.040	4.290	0.767	4.243	0.764
197	NO CADMIUM - Poly on SNAP	2.646	3.655	0.726	3.046	4.300	0.767	4.221	0.763
163	NO CADMIUM - NO Poly on SNAP	2.656	3.670	0.728	3.048	4.303	0.768	4.239	0.764
200	NO Cd OR POLY - Poly on SNAP	2.637	3.640	0.725	3.025	4.266	0.766	4.243	0.764
165	NO Cd OR POLY - NO Poly on SNAP	2.648	3.658	0.727	3.021	4.259	0.765	bad data	--

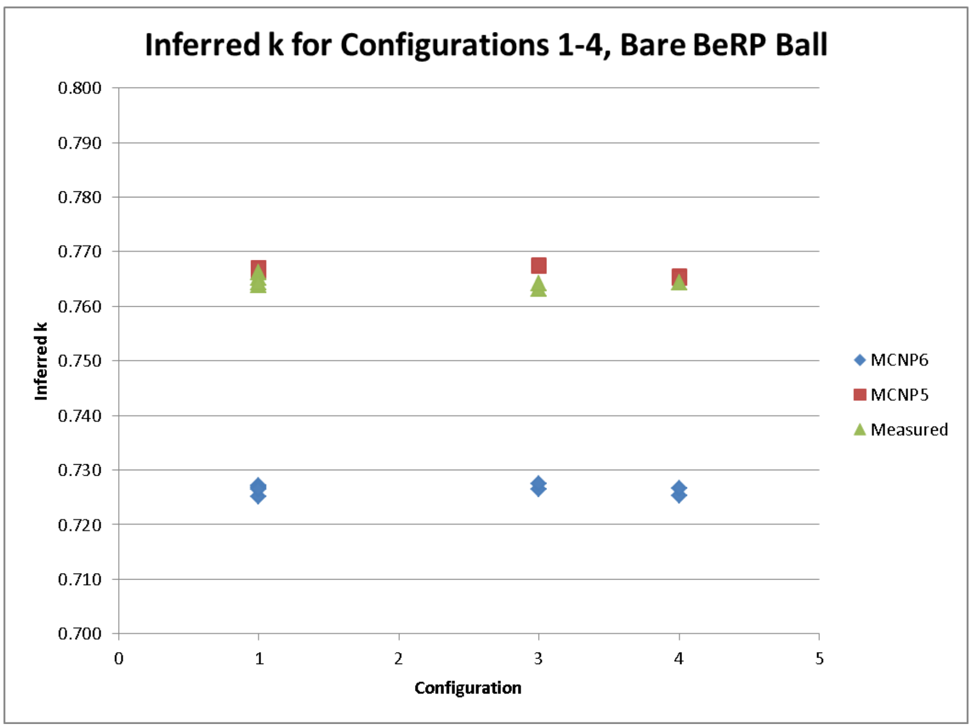

Figure 4: Plot of inferred k versus configuration for simulated and measured data.

Conclusion

The simulated results show no difference in response when one NPOD is in various states of disassembly. Even for Configuration 4 with the Cd and the polyethylene removed from one of the detectors, the count rate remains unchanged because the unmoderated detector records very few counts, so few that they are statistically insignificant. As long as one detector is in a complete, functioning state, and room return is insignificant, the multiplication as measured by the detectors should not vary for a bare source since multiplicity is inherent in the way the counts are distributed, not in the total number of counts. Future work will involve modeling the remaining detector configurations and including the reflected BeRP ball cases to see if a difference can be seen as multiplication increases. Also, the detectors will be tallied separately, as was done in the measurements.

The results from the MCNP5/list mode patch calculations show excellent agreement with the measured results, with a difference ranging from 0.4% to 1.8% in the total multiplication. The MCNP6 results, on the other hand, are approximately 16% lower than the other results. The cause of the lower inferred k values for MCNP6 is most likely due to the treatment of the time stamp in the PTRAC file, which is explained below.

It was noticed in the simulations that the fission spectrum used for the source definition has a fairly significant effect on the results. When a generic Pu-240 Watt fission spectrum is used, the total multiplication values were higher than when the SOURCES4C time-corrected spectrum was used. The source definition will be revisited to determine the accuracy of the spectrum used.

One discrepancy that perhaps exists within the NPOD model is the active length and the pressure of the gas in the He-3 tubes. These properties have been estimated, but the actual data are proprietary to the manufacturer of the tubes. An overestimate of the pressure and/or an overestimate of the active length could lead to a slightly higher inferred k value as seen in this and previous calculations. A sensitivity study of the effect of He-3 density and active length will be conducted.

MCNP6's PTRAC option is not an ideal method for obtaining list-mode data. While it does provide time-tagged neutron interactions within the detectors as desired, it has several limitations, the most significant being the inability to run a PTRAC calculation in parallel. The calculation time for list-mode simulations can be long since they must be run in analog mode (variance reduction does not currently exist for these calculations), where the ability to run in parallel is very beneficial.

The other primary drawback to utilizing the PTRAC as a source of list-mode data is the lack of precision in the time stamp. It is limited to five digits, where the measured list-mode data and the output from MCNP5 with the patch provide the time with five digits after the decimal. As an example, the PTRAC time would be shown as 0.11694E+11 (converted to 11694000000.00000 by the parsing script to match the detector output format); the "equivalent" time as given by MCNP5 w/patch would be 11694946207.32986 (time is given in shakes or 10E-8 seconds). This is the probable cause of the significant difference in the results from the MCNP5 and the measured values since the lack of precision results in fewer events being correlated.

A third limitation is the necessity for a parsing script to modify the PTRAC file into the correct format. As it stands, when using the capture option for the EVENT keyword for the PTRAC file, the raw output provides the time from the source event to the time of capture, not the time from the beginning of measurement to the time of capture as is done in standard list-mode data collection. The script adds the time from the beginning of measurement to the time of the source event, removes superfluous data, and rearranges the data columns to mimic the output of the NPODs. Other PTRAC output options are currently being investigated (such as replacing the capture option with a termination option, which records the time from the beginning of the measurement to the time of absorption in the detector (termination). Currently, the results using the termination option are significantly incorrect, so other keyword combinations must be used).

Another question that has yet to be answered is the reason behind the increase in the bias of the simulated results as the reflector thickness is increased. Previous papers have looked into this and concluded that the error does not lie in an incorrect definition or data for the polyethylene [6,7]. They posited that the source of the error may lie in the definition of nubar (the average number of neutrons produced per fission event) for Pu-239. This topic will be approached when the reflected cases are analyzed.

References

K. Clark, A. Sood, B. Myers, J. Hutchinson, D. Beller. “Comparison of MCNP-based transport codes for subcritical calculations”. American Nuclear Society Winter Meeting, San Diego, 2012.

W. Wilson, R. Perry, W. Charlton, E. Shores, T. Parish. “SOURCES4C: A code for calculating (alpha,n), spontaneous fission, and delayed neutron sources and spectra”. Los Alamos National Laboratory, LA-UR-02-1839, 2002.

C. Solomon. “Modifications to the MCNP5 multiplication patch”. Los Alamos National Laboratory, LA-UR-11-04711, 2011.

D. Pelowits. “MCNP6 user’s manual”. Los Alamos National Laboratory, LA-CP-11-01708.

M. Chadwick, et al. “ENDF/B-VII.1 nuclear data for science and technology: cross sections, covariances, fission product yields and decay data.” Los Alamos National Laboratory, LA-UR-11-05121, 2011.

S. Bolding, C. Solomon. “Simulations of multiplicity distributions with perturbations to nuclear data”. American Nuclear Society Winter Meeting, Washington, D.C., 2013.

E. Miller, J. Mattingly, et al. “Simulations of neutron multiplicity measurements with MCNP-PoliMi”. Sandia National Laboratory, SAND2010-6830.